Immediate Early Effector Functions of Virus-Specific CD8$^+$CCR7$^+$ Memory Cells in Humans Defined by HLA and CC Chemokine Ligand 19 Tetramers

Eugene V. Ravkov, Christy M. Myrick and John D. Altman

References
This article **cites 30 articles**, 19 of which you can access for free at:
http://www.jimmunol.org/content/170/5/2461.full#ref-list-1

Why *The JI*? Submit online.

- **Rapid Reviews! 30 days*** from submission to initial decision

- **No Triage!** Every submission reviewed by practicing scientists

- **Fast Publication!** 4 weeks from acceptance to publication

*average

Subscription
Information about subscribing to *The Journal of Immunology* is online at:
http://jimmunol.org/subscription

Permissions
Submit copyright permission requests at:
http://www.aai.org/About/Publications/JI/copyright.html

Email Alerts
Receive free email-alerts when new articles cite this article. Sign up at:
http://jimmunol.org/alerts

Immediate Early Effector Functions of Virus-Specific CD8+CCR7+ Memory Cells in Humans Defined by HLA and CC Chemokine Ligand 19 Tetramers[1]

Eugene V. Ravkov, Christy M. Myrick, and John D. Altman[2]

Memory T cells exhibit a high degree of heterogeneity in terms of their phenotype and functional characteristics. It has been proposed that the CCR7 chemokine receptor divides memory T cell populations into central memory T cells and effector memory T cells with distinct functions in secondary immune responses. We were interested whether this hypothesis holds true in experiments performed on Ag-specific CD8+ T cells. To identify CCR7+ cells, we engineered a fluorescent ligand for CCR7; results with the new CC chemokine ligand 19 chemotetramer were verified by staining with a CCR7 mAb. Staining with the CC chemokine ligand 19 chemotetramer reveals two subsets within CCR7+ cells: a CCR7int population containing memory cells and a CCR7high population containing naive T cells. Phenotypic analysis of MHC class I/peptide tetramer-positive cells revealed that HLA-A2-restricted CMV-specific CD8 T cells exhibit the lowest percentage of CCR7+ cells (0.5–5%), while HLA-A2-restricted flu- and HLA-B8-restricted EBV-specific CD8 T cells showed the highest (45–70%). Intracellular staining of unstimulated cells revealed that both CCR7int- and CCR7−-specific CD8 T cells exhibit a detectable level of perforin. Both CCR7int and CCR7− Ag-specific CD8+ T cells produced IFN-γ and TNF-α following short-term peptide stimulation. Therefore, our finding that CCR7+CD8+ T cells are able to exert immediate effector functions requires a substantial revision to the central and effector memory hypothesis. *The Journal of Immunology,* 2003, 170: 2461–2468.

O ver the last 5 years, the characterization of the phenotypic heterogeneity of bulk memory T cell populations has been extended to Ag-specific CD8+ memory populations defined by class I MHC tetramer staining (1). To a great extent, both the causes and consequences of the phenotypic heterogeneity of populations of Ag-specific T cells remain poorly understood, despite the considerable efforts that have gone into delineating and characterizing the populations.

A number of recent studies have shown that populations of Ag-specific T cells defined by MHC tetramer staining are not only phenotypically heterogeneous, they also exhibit apparent functional heterogeneity (2–6). Almost all of these studies have focused upon class I MHC-restricted CD8+ T cells in humans—because the relevant tetramers are available, and because the cells are present at a sufficiently high frequency to permit robust analyses—and have compared the frequency of cells defined by tetramer staining to the frequency of cells that are detectable by intracellular cytokine staining of cells stimulated with peptide Ags for 4–12 h. A few investigators have also attempted to correlate results obtained from tetramer staining to lytic function (2, 3, 7).

Many investigators have concluded that functional heterogeneity reflects genuine biological differences between distinct subpopulations (3–6, 8), and many have interpreted their findings in terms of the central and effector memory hypothesis proposed by Sallusto et al. (9). The central and effector memory hypothesis proposes that there are two major subpopulations of memory T cells. Central memory T cells (T_{CM})[3] efficiently home to lymph nodes due to expression of CCR7 and CD62L and may have a high proliferative potential, but they are not capable of immediate effector functions such as cytokine secretion or cytotoxicity. In contrast, effector memory T cells (T_{EM}) lack expression of CCR7, but they are capable of immediate effector functions, presumably permitting them to act early during a secondary immune response in nonlymphoid tissues.

The primary objective of our studies was to examine whether the central and effector memory hypothesis could account for the functional heterogeneity of Ag-specific CD8+ T cells in humans. Our approach was to identify CCR7+ populations of Ag-specific CD8+ T cells by staining with HLA tetramers, and to determine whether these were capable of immediate effector function using the intracellular cytokine staining assays. When we began these studies, an anti-CCR7 Ab was not available to us. Therefore, we implemented a strategy to identify CCR7+ cells by staining with a CCR7 ligand, CC chemokine ligand (CCL)19 (also known as macrophage-inflammatory protein-3β, EBV-induced molecule-1 ligand chemokine, or exodus-3 (10, 11)), using the same biotin labeling strategy for the chemokine that we use for MHC tetramers (1). In this study, we demonstrate the specificity of the CCL19 chemotetramer and its usefulness in the identification of CCR7 phenotypes in humans. Most importantly, we show that CCR7int Ag-specific CD8+ T cells are potent producers of effector cytokines in short-term, intracellular cytokine staining assays. In addition, intracellular staining of unstimulated cells revealed that CCR7int virus-specific CD8 T cells exhibit a detectable level of

Department of Microbiology and Immunology, and Emory Vaccine Research Center at Yerkes, Emory University, Atlanta, GA 30329

[2] Address correspondence and reprint requests to Dr. John D. Altman, Emory Vaccine Research Center at Yerkes, 954 Gatewood Road, Atlanta, GA 30329. E-mail address: altman@microbio.emory.edu

[3] Abbreviations used in this paper: T_{CM}, central memory T cell; T_{EM}, effector memory T cell; CCL, CC chemokine ligand; IPTG, isopropyl β-D-thiogalactoside.

perforin. These results demonstrate that the functional heterogeneity of Ag-specific CD8$^+$ T cells is not correlated with the CCR7 (or CD62L) phenotype, contradicting some recent reports (2, 6), while agreeing with others (4, 12). They also raise cautionary questions about important features of the central and effector memory hypothesis (9).

Materials and Methods

Donors and samples

Samples were obtained from 16 healthy individuals. The blood samples were provided in either heparin- or EDTA-anticoagulant tubes. PBMC were isolated from the blood samples over lymphocyte-separation medium (Cellgro, Herndon, VA). In few cases, cryopreserved PBMC were used.

MHC class I/peptide tetramers

Soluble MHC class I/peptide tetramers carrying CTL epitopes of CMV, EBV, and flu proteins were produced as described elsewhere (1). The HLA restriction, peptide sequences, the virus, and the name of the gene products of derived CTL epitopes are presented in Table I. The tetramers were prepared with streptavidin coupled to either allophycocyanin or PE (Molecular Probes, Eugene, OR).

Construction of pET-CCL19/BSP41 plasmid and expression of CCL19 monomer

The cDNA sequence for mature human CCL19 chemokine was produced by PCR amplification with primers CCL19.5P (5′-GGAATTCCATATGG GAACAAATGATGCTGAAGACTGC-3′) and CCL19.3P (5′-CGGGAT CCACTGCTGCGGCGCTTCAT-3′), using the plasmid AI-pTyT30 (Incyte Genomics, St. Louis, MO) as a template. CCL19.5P contains *Nde*I-restrictase adapter sequence, followed by the initiating ATG codon and the nucleotides complementary to the 5′ portion of the CCL19 coding sequence. CCL19.3P contains *Bam*HI-restrictase adapter sequence and nucleotides complementary to the 3′ portion of the CCL19 coding sequence preceding the stop TAA codon. The amplified DNA fragment was digested with *Nde*I and *Bam*HI and inserted into the pJA1 plasmid linearized with the same enzymes. In this construct, the nucleotide coding sequence for mature CCL19 was placed downstream of T7 promoter and upstream of the BSP41 biotinylation site coding sequence followed by a TGA stop codon. The orientation of the insert and its sequence authenticity were verified by nucleotide sequence analysis. The resulting plasmid pET-CCL19/BSP41 directs the synthesis of a CCL19 protein fused with 17 aa of BSP41 biotinylation site in *Escherichia coli* regulated by the isopropyl β-D-thiogalactoside (IPTG)-inducible T7 promoter. *E. coli* strain BL21 (DE3) was transformed with pET-CCL19/BSP41 and analyzed for CCL19 monomer expression by SDS-PAGE on a small-scale culture according to the pET system manual (Novagen, Darmstadt, Germany). The majority of the protein (~65% of total sample) was expressed after 4 h of IPTG induction in the form of inclusion bodies. The protein migrated as the major band at 11 kDa.

Preparation of CCL19 chemotetramer

CCL19 monomer was prepared from 6 L of *E. coli* culture. The cells were collected by centrifugation after 4 h of IPTG induction and sonicated in 50 ml of resuspension buffer (50 mM Tris-HCl (pH 8.0), 25% sucrose, 1 mM EDTA (pH 8.0), 10 mM DTT, 1 mg/ml lysozyme, 5 mM MgCl$_2$, and 0.4 mg/ml DNase I). The insoluble material was collected by centrifugation at 20,000 × *g* for 10 min and washed four times in wash buffer with Triton X-100 (50 mM Tris-HCl (pH 8.0), 0.5% Triton X-100, 2 M urea, 1 mM EDTA, and 1 mM DTT) and one time in wash buffer without Triton X-100. The insoluble material was collected by centrifugation and dissolved in extraction buffer (8 M guanidine-HCl, 50 mM Tris-HCl (pH 7.4), 5 mM EDTA, and 5 mM DTT). CCL19 monomer was purified by gel filtration chromatography on a S100 column (Amersham-Pharmacia, Piscataway, NJ) in gel filtration buffer with guanidine-HCl (50 mM Tris-HCl (pH 7.5), 4 M guanidine-HCl, and 2 mM DTT). The protein purity was >99%. The denatured protein (20 mg) was folded in 1 L of folding buffer (400 mM L-arginine, 100 mM Tris-HCl (pH 8.3), 2 mM EDTA, 5 mM reduced glutathione, and 0.5 mM oxidized glutathione) at 10°C for 72 h. The folding reaction was concentrated to the volume of 7.5 ml by ultrafiltration, using a Biomax 5000 membrane in an Amicon 500-ml stir cell (Millipore, Bedford, MA) and exchanged against biotinylation buffer (100 mM Tris (pH 7.5), 200 mM NaCl, and 5 mM MgCl$_2$) on a PD-10 column (Amersham-Pharmacia). The folded CCL19-BSP41 (10.5 ml) in biotinylation buffer was mixed with 500 μl of 100 mM ATP, 40 μl of 100 mM biotin, 10 μl

of leupeptin, 10 μl of pepstatin, 20 μl of 100 mM PMSF, and 10 μl of BirA (20 μg), and incubated overnight at room temperature. The biotinylated CCL19 monomer was purified by gel filtration on a S100 column in gel filtration buffer without guanidine-HCl and DTT (50 mM Tris-HCl (pH 7.5) and 150 mM NaCl). The appropriate fractions were collected, concentrated in an ultrafree-15 centrifuge filtering tube, and dialyzed three times against 1 L of PBS without Ca and Mg (Cellgro). The CCL19 monomer was adjusted to 2 mg/ml, sampled into 10-μl aliquots, and stored at −80°C. The CCL19 monomer (10 μl) was incubated with a total of 32.4 μl of PE-streptavidin or 18 μl of allophycocyanin-streptavidin (Molecular Probes) for 1 h and 40 min at room temperature.

Intracellular cytokine staining

PBMC (1 × 10^6 cells) were stimulated with an appropriate peptide (10 μg/ml) in 1 ml of RPMI 1640/10% FBS medium, containing costimulatory Abs CD28 (1 μg/ml) and CD49d (1 μg/ml) and GolgiPlug (BD PharMingen, San Diego, CA) for 6 h at 37°C. After peptide stimulation, intracellular cytokine staining was conducted using Cytofix/Cytoperm Plus kit (BD PharMingen). Peptide-stimulated PBMC were stained with CD8-PerCP for 15 min at 4°C, washed twice with 2 ml of FACS buffer (PBS and 2% BSA). The cells were permeabilized with Cytofix/Cytoperm, washed twice with Perm/Wash buffer, stained with IFN-γ-FITC, TNF-α-PE, and CD3-allophycocyanin for 15 min at 4°C, washed again, and fixed with 1% paraformaldehyde before acquisition of the data on a FACSCalibur (BD Biosciences, Mountain View, CA). FACS data were analyzed with FlowJo software (Tree Star, San Carlos, CA).

Intracellular staining for perforin and granzyme B

Freshly prepared PBMC (1 × 10^6 cells/100 μl) were preincubated in a cell surface staining buffer (10% FBS and PBS) for 40 min at 4°C and then stained with cell surface Abs and reagents (CD8-PerCP, CCL19-tet-PE, CD3-allophycocyanin, or MHC/peptide tetramers) for 15 at 4°C. Cells were washed in the cell surface staining buffer twice and then permeabilized and stained with intracellular Abs following Cytofix/Cytoperm Plus kit protocol (BD PharMingen) in a 96-well plate. Perforin FITC Ab was purchased from BD PharMingen. Granzyme B allophycocyanin Ab was purchased from Caltag (Burlingame, CA).

Immunophenotyping of lymphocytes

Cells were stained with FITC-, PE-, PerCP-, and allophycocyanin-labeled Abs or tetramers, using standard methods. Any remaining free biotin binding sites in PE- and allophycocyanin-labeled tetramers were quenched by the addition of biotin (1 mM), followed by incubating for 30 min on ice before staining cells. The whole blood samples (200 μl) were stained at room temperature for 15 min; RBCs were lysed in FACS lysing solution (BD Biosciences) for 10 min, washed twice in FACS buffer, and fixed in 200 μl of 1% paraformaldehyde. PBMC (1 × 10^6 cells/100 μl) were stained at 4°C for 15 min, washed twice with 2 ml of FACS buffer, and fixed with paraformaldehyde. The following FITC-labeled Abs (Beckman Coulter, Fullerton, CA) were used: CD3, CD11a, CD16, CD45RA, CD56, and CD62L. CD8-PerCP and unlabeled CCR7 IgM were purchased from BD Biosciences. The mAbs CD20-allophycocyanin and CD3-allophycocyanin were obtained from Beckman Coulter. Staining with unlabeled CCR7 Ab was detected by a secondary anti-mouse-FITC Ab (Jackson ImmunoResearch, West Grove, PA).

Results

Generation of CCL19 chemotetramer

CCR7 has two functional ligands, one of which, CCL19, appears to signal exclusively through CCR7 in both mouse and human cells (13). Because the appropriate mAb to human CCR7 was not available at the initiation of this study, we engineered a CCL19 chemotetramer, using the same methodology that we use to produce MHC/peptide tetramers (1), with the purpose of using it as a staining reagent for phenotypic characterization of Ag-specific CD8$^+$ T cells. Fig. 1, *A* and *B*, shows CCL19 chemokine staining on four major subsets of PBMC in humans. No staining is observed on CD16$^+$CD56$^+$ lymphocytes, representing NK cells, and a moderate level of it is seen on nearly all B cells, identified as CD20$^+$. The populations of CD3$^+$CD4$^+$ and CD3$^+$CD8$^+$ exhibit the highest level of CCL19 chemotetramer staining, with more CD3$^+$CD4$^+$ than CD3$^+$CD8$^+$ cells staining positive with the
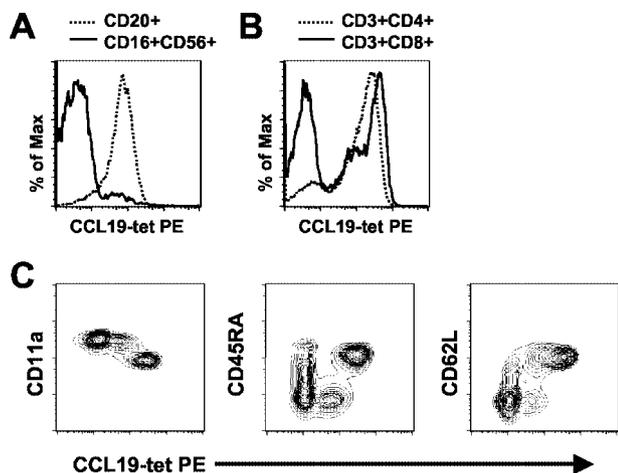
FIGURE 1. CCL19 chemotetramer staining on lymphocytes. *A* and *B*, CCL19 chemotetramer staining on four defined subsets of lymphocytes. PBMCs were prepared from a blood sample of a healthy donor (donor 20) and stained with a panel of Abs and CCL19 chemotetramer-PE on the same day in two separate tubes (*A* and *B*). *A*, Shown is a histogram of cells stained with and gated on CD20-allophycocyanin (dashed line) and CD16-FITC plus CD56-FITC (solid line) lymphocytes that were plotted for CCL19 chemotetramer-PE fluorescence (*x*-axis). *B*, Shown is CCL19 chemotetramer-PE fluorescence of stained cells that were gated on CD3-allophycocyanin plus CD8-PerCP- (solid line) and CD3-allophycocyanin plus CD4-FITC- (dashed line) positive populations. *C*, Shown is CCR7 expression on CD3$^+$CD8$^+$ lymphocyte subsets analyzed by CCL19 chemotetramer staining and T cell markers. The whole blood samples (donor 20) were stained with CD8-PerCP, CCL19 chemotetramer-PE, and one of the following markers: CD11a-FITC (*left*), CD45RA-FITC (*center*), and CD62L-FITC (*right*). The cells are lymphocytes gated on CD8^{high} subsets. CCL19 chemotetramer-PE staining is shown on the *x*-axis.

CCL19 tetramer. Within the CD3$^+$CD8$^+$ population, CCL19 chemotetramer-positive cells can be divided into intermediate and high subsets.

We also performed costaining of PBMC with the CCL19 chemotetramer and CCR7 mAb, which became available during the course of this study, and showed that both reagents bind to the same subsets of CD3$^+$CD8$^+$ and CD3$^+$CD8$^-$ cells. In addition, preincubation of PBMC with increased concentrations of CCR7 mAb completely abrogated CCL19 chemotetramer binding on CD3$^+$CD4$^+$ and CD3$^+$CD8$^+$ cells (data not shown), indicating that the CCL19 chemotetramer binds to CCR7 in a specific manner.

Phenotypic characterization of the bulk population of CD8 T cells

CCL19 chemotetramer staining on CD3$^+$CD8$^+$ cells identifies three subsets of cells: CCR7$^-$, CCR7^{int}, and CCR7^{high} (Fig. 1*B*). We further characterized these subsets by performing immunophenotypic analyses of bulk CD3$^+$CD8$^+$ cells by costaining with the CCL19 chemotetramer and a panel of markers of naive and Ag-

experienced CD8 T cells. Staining with CD11a, a human T cell marker for Ag-experienced cells, identifies all cells within the CCR7^{int} subset as bright and those within the CCR7^{high} subset as dull (Fig. 1*C*). The same exact pattern was observed with CD95 Ab (data not shown). In contrast, staining with CD45RA Ab, traditionally used as a marker of naive T cells, shows that the CCR7^{high} subset is exclusively CD45RA^{bright} and the CCR7^{int} subset is predominantly CD45RA$^-$, with a fraction of cells seen as CD45RA^{dull}. Discrimination with respect to CD62L, another marker for naive T cells, shows a somewhat similar pattern. Taken together, these results indicate that the level of CCR7 present on CD8$^+$ T cells allows discrimination between the memory population, which is CCR7^{int}, and the naive T cell population, which is CCR7^{high}.
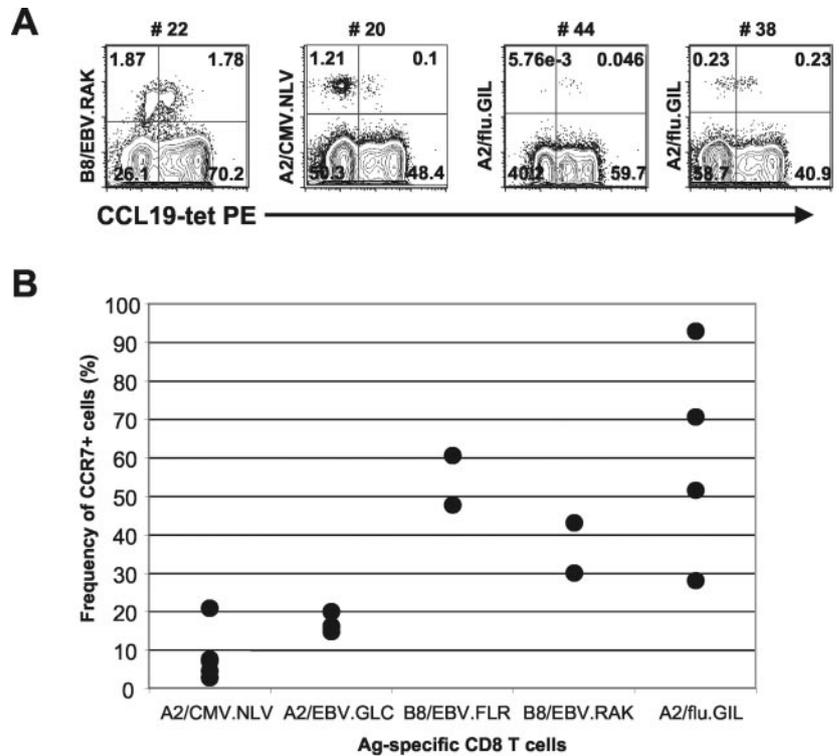
Expression of CCR7 on Ag-specific CD8 T cells

Unlike primary effector T cells, memory CD8 T cells exhibit a high degree of heterogeneity in terms of their cell surface markers and their functional characteristics. We were interested in examining whether this heterogeneity could be delineated with respect to CCR7 expression on the Ag-specific CD8 T cells specific for both latently persistent and rapidly cleared viral infections in humans. To address this question, we used five MHC class I/peptide tetramers that bear peptides from CMV, EBV, and flu viral Ags, and are restricted by either the HLA-A2 or the HLA-B8 (Table I). A2/EBV.GLC and B8/EBV.RAK tetramers recognize T cells specific for CTL epitopes of BMLF1 and BZLF1 EBV Ags, respectively (14). B8/EBV.FLR is an antigenic determinant of EBNA3A EBV protein and is presented by HLA-B8 during virus latency (14). A2/CMV and A2/flu.GIL tetramers recognize HLA-A2-restricted epitopes of CMV pp65 and influenza MP proteins, respectively.

The staining with MHC class I/peptide tetramer and CCL19 chemotetramer was conducted on whole blood samples collected from 12 healthy HIV$^-$ donors. Fig. 2 shows that the frequencies of CCR7$^+$ cells in the MHC class I/peptide tetramer-positive cells used in this analysis vary significantly. However, regardless of what type of infection the Ag is associated with, or the MHC class I restriction, the Ag-specific CD8 T cell populations contain only CCR7$^-$ or CCR7^{int} cells, consistent with the results of the previous section that demonstrated that the CCR7^{high} phenotype is restricted to naive cells.

There is a substantial and variable degree of heterogeneity of CCR7 expression between cells specific for different viruses and Ags and between different donors. The CMV-specific CD8 T cells exhibit the lowest percentage of CCR7$^+$ cells, while A2/flu.GIL cells demonstrate the highest (Fig. 2*B*). The difference in the percentage of CCR7$^+$ cells in HLA-A2-restricted epitopes appears to be attributable to the type of viral infection (i.e., latently persistent vs rapidly cleared) rather than to the type of MHC class I restriction or an anticipated variability between donors.

Table I. *MHC class I/peptide tetramers and HLA-restricted epitopes*

MHC/Peptide Tetramers	HLA Restriction	CTL Epitope	Viral Infection	Viral Protein
A2/CMV	A*0201	NLVPMVATV	CMV	pp65
A2/flu.GIL	A*0201	GILGFVFTL	flu	MP
A2/EBV.GLC	A*0201	GLCTLVAML	EBV	BMFL1
B8/EBV.FLR	B*0801	FLRGRAYGL	EBV	EBNA3A
B8/EBV.RAK	B*0801	RAKFKQLL	EBV	BZLF1

FIGURE 2. Expression of CCR7 on Ag-specific CD8 T cells. Staining was performed on the whole blood samples obtained from healthy donors. The panel of staining reagents included CCL19 chemotetramer-PE, CD8-PerCP, and one of the following MHC class I/peptide allophycocyanin-labeled tetramers: A2/CMV, A2/EBV, A2/flu, B8/EBV.FLR, and B8/EBV.RAK (Table I). Both CCL19 chemotetramer-PE and each of the MHC class I/peptide-allophycocyanin tetramers were quenched with 1 mM biotin for 30 min on ice prior to cell staining. The lymphocytes were gated on CD8^{high} subset of cells and plotted for CCL19 chemotetramer-PE (x-axis) and each of the MHC class I/peptide-allophycocyanin tetramers (y-axis). The number of each donor is indicated above the plots. *B,* Shown is the heterogeneity of CCR7 expression in CD8 T cells specific for different viral Ags in different donors. Each dot represents an average percentage of CCR7^{int} Ag-specific CD8 T cells determined in five independent experiments in various donors.

CCR7$^+$ Ag-specific CD8 T cells are capable of secreting effector cytokines within a short time of stimulation

The hypothesis of central and effector memory T cells derives from studies conducted on a polyclonal populations of T cells with different Ag specificities, whose functional responses were measured using the bacterial superantigen toxic shock syndrome toxin, CD3 mAb, or PMA/ionomycin activators (9). Therefore, it was imperative to examine whether this hypothesis holds true in experiments performed on Ag-specific CD8 T cells, stimulated in an Ag-specific manner.

We reasoned that the percentage of CCR7$^-$ cells on Ag-specific CD8 T cells before stimulation would correlate with the frequencies of cells capable of producing effector cytokines in a short-term Ag stimulation assay. Fig. 3, *A*, *B*, and *C*, shows intracellular cytokine staining for IFN-γ in the B8/EBV.RAK, B8/EBV.FLR, and A2/flu.GLC-specific CD8 T cells from donor 42 that were stimulated with corresponding peptides (Table I) for 6 h. In this donor, the frequency of B8/EBV.RAK-specific CD8 T cells positive for CCR7 is 31.2%. Despite this significant number of CCR7$^+$ cells, nearly all of the B8/EBV.RAK-specific CD8 T cells (90.3%) produce IFN-γ. Similarly, IFN-γ production in B8/EBV.FLR and A2/flu-specific CD8 T cells of this donor after peptide stimulation is also at much higher levels than that predicted from the frequencies of CCR7$^-$ cells prior to stimulation (Fig. 3, *B* and *C*). The same pattern was observed for TNF-α (data not shown). This indicates that CCR7$^+$ Ag-specific CD8 T cells are able to express effector cytokines in a short-term Ag stimulation assay. This feature is not limited to this particular donor. Fig. 3*D* shows IFN-γ production in B8/EBV.FLR CD8 T cells from donor 22. In this study, too, the frequencies of IFN-γ-producing cells were much higher as compared with the percentage of CCR7$^-$ Ag-specific CD8 T cells.

Thus, our results suggest that both CCR7$^+$ and CCR7$^-$ Ag-specific CD8 T cells are capable of rapid expression of effector cytokines. Therefore, it appears that the division of memory CD8 T cells into T$_{CM}$ and T$_{EM}$ according to the CCR7 expression and the ability to produce effector cytokines requires substantial revision. Unsoeld et al. (12) have come to similar conclusions in mouse models.

Donor 22 had a high frequency of B8/EBV.RAK-specific CD8$^+$ T cells, comprising 1% of the total population of lymphocytes, and ~50% of the epitope-specific cells express CCR7. Fig. 4*A* shows the CCR7 phenotype of unstimulated B8/EBV.RAK-specific CD8 T cells from donor 22 (*left panel*). Peptide stimulation (10 μg/ml) reveals that only one-third of the total B8/EBV.RAK cell population are potent immediate producers of IFN-γ (data not shown). It is noteworthy to mention that Ag stimulation of these cells using higher peptide concentrations had resulted in the greater frequencies of IFN-γ-producing cells (data not shown). To examine the relationship between the CCR7 phenotype of the unstimulated CD8$^+$ T cells and the ability of these cells to produce effector cytokines, freshly prepared PMBC from donor 22 were stained with the B8/EBV.RAK tetramer and the CCL19 chemotetramer and then FACS sorted into B8/EBV.RAK$^+$CCR7$^+$ and B8/EBV.RAK$^+$CCR7$^-$ subsets. Subsequently, we tested the ability of the sorted cells to produce IFN-γ in a 6-h stimulation assay, using peptide-pulsed autologous B lymphoblastoid cell lines as stimulators. (Fig. 4*B*). The *left panel* in each row shows the lack of IFN-γ production before stimulation; panels to the *right* represent peptide-stimulated cells. It can be seen that both CCR7$^-$- and CCR7^{int}-sorted B8/EBV.RAK-specific CD8 T cells express IFN-γ at the same frequency (~30%). The data in Fig. 4 are representative of three independent experiments. Similar results were also obtained with TNF-α production (data not shown). The lack of bias in the production of effector cytokines between CCR7$^-$ and CCR7$^+$ CD8 T cells indicates that cells with a surface phenotype previously ascribed to T$_{CM}$ are in fact capable of at least one immediate effector function, and that the heterogeneous potential of B8/EBV.RAK cells in donor 22 (Fig. 4*A*) is not accounted for by the CCR7 phenotype.

Expression of perforin in Ag-specific CD8 T cells

Although IFN-γ and TNF-α are important players in the clearance of infected targets, the most significant molecules mediating this process are perforin and various isoforms of granzymes (15). The

FIGURE 3. The ability of CCR7+ Ag-specific CD8 T cells to produce IFN-γ. Freshly prepared PBMCs from donors 42 (*A, B,* and *C*) and 22 (*D*) were stimulated with a panel of peptides (Table I) for 6 h in the presence of brefeldin A and examined for IFN-γ production by intracellular staining assay. The *left diagram* in each panel shows unstimulated CD3+CD8+ gated lymphocytes that are plotted for MHC class I/peptide tetramer (*y*-axis) and CCL19 chemotetramer stains (*x*-axis). The diagram situated in the *center* of each panels represents unstimulated CD3+CD8+ cells with stains for MHC class I/peptide tetramer (*y*-axis) and IFN-γ (*x*-axis). The diagrams to the *right* are peptide-stimulated CD3+CD8+ gated lymphocytes showing expression of IFN-γ (*x*-axis) and residual staining for MHC class I/peptide tetramer (*y*-axis). *A* and *B,* Shown are B8/EBV.RAK and A2/flu Ag-specific CD8 T cells, respectively, from donor 42. *B* and *D,* Shown are B8/EBV.FLR Ag-specific CD8 cells from donors 42 and 22, respectively.
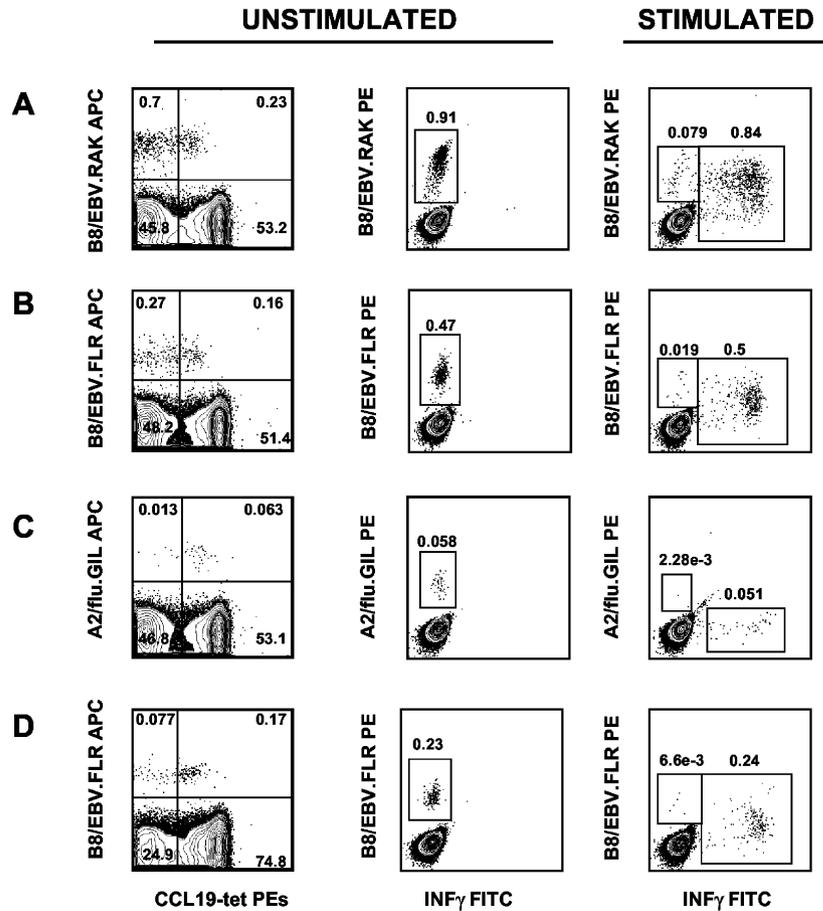

central and effector memory hypothesis states that CCR7+ memory CD8 T cells are largely devoid of these effector molecules before antigenic stimulation, while CCR7− memory cells do express them (determined by immunofluorescence assay) (9).

We were interested in examining the relationship between CCR7 and perforin and granzyme B in both the bulk population of CD8 T cells and epitope-specific CD8 T cells in healthy donors. Fig. 5A shows CD3+CD8+ lymphocytes (donor 68) stained for perforin and CCR7. Overall, it appears that there is an inverse correlation between CCR7 and perforin, consistent with the original observations

of Sallusto et al. (9). However, a closer look allows identification of five distinct subsets. CCR7bright cells, identified previously as naive cells, are completely devoid of perforin. CCR7int cells, described as central memory CD8 T cells, express perforin either at low or high levels. CCR7− cells, representing populations of memory and effector CD8 T cells, can be divided with respect to perforin into intermediate and high subsets. The frequencies of these five subsets vary from donor to donor (data not shown).

Granzyme B also exhibits an inverse correlation with CCR7; however, for unknown reasons and despite much effort, we have
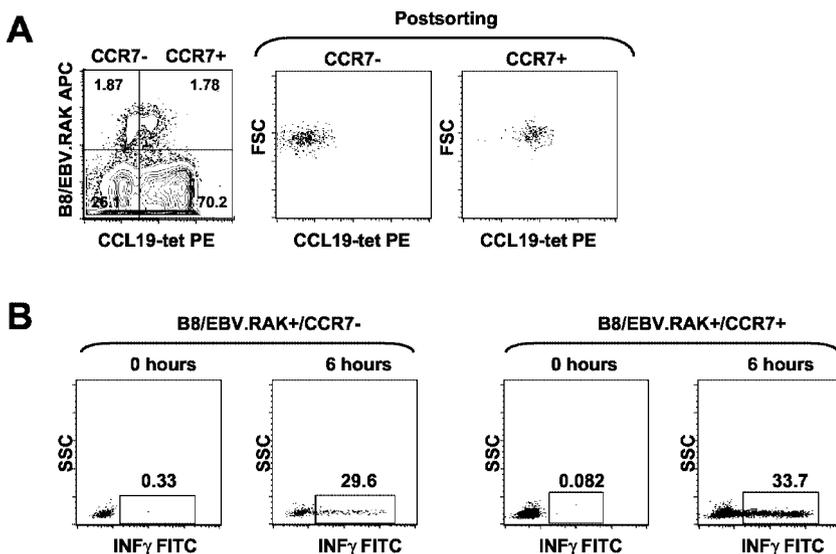
FIGURE 4. CCR7+ CD8 memory T cells are potent immediate producers of IFN-γ. *A,* Shown is a comparison between CCR7 phenotype and IFN-γ production upon peptide stimulation in PBMCs from donor 22. In the *far left panel,* freshly prepared PBMC were stained with CD3-FITC, B8/EBV.RAK-allophycocyanin, CD8-PerCP, and CCL21 chemotetramer-PE. Lymphocytes were gated on CD3+CD8+ cells and plotted on B8/EBV.RAK+ and CCL21 chemotetramer+ cells. The panels in the *middle* and to the *right* of the row show the quality of FACS sorting. *B,* Shown is IFN-γ production in B8/EBV.RAK+CCR7+ and B8/EBV.RAK+CCR7− cells prior to (*left panels*) and after (*right panels*) peptide stimulation. Peptide-loaded B lymphoblastoid cell line cells were gated out by the size and granularity and by the lack of CD3-allophycocyanin that was added intracellularly after peptide stimulation of the sorted cells.
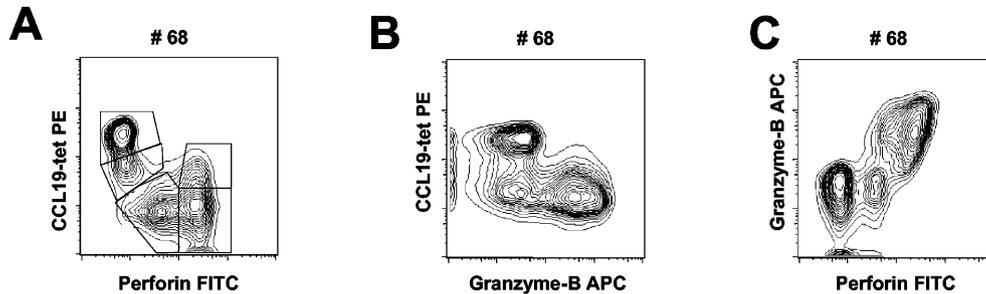
FIGURE 5. Expression of perforin, granzyme B, and CCR7 in the bulk population of CD8 T cells. *A*, CD3$^+$CD8$^+$ gated lymphocytes from donor 68. The *y*-axis shows expression of CCR7, and the *x*-axis is perforin. Five distinct subsets can be identified: CCR7^{high}perforin$^-$, CCR7$^-$perforin^{high}, CCR7$^-$perforin^{low}, CCR7^{int}perforin^{high}, and CCR7^{int}perforin^{low}. *B* and *C*, Shown is the relationship between CCR7 and granzyme B, and between granzyme B and perforin, respectively, in CD3$^+$CD8$^+$ cells.

been unable to resolve the CCR7^{int} and CCR7^{high} subsets (Fig. 5*B*). In addition, we observed distinct patterns of perforin and granzyme B in CD8 T cells (Fig. 5*C*). Nearly half of the examined donors showed the presence of perforin$^+$granzyme B$^-$ subsets, and no perforin$^-$granzyme B$^+$ cells were observed. The pattern of staining is very sensitive to details of the protocol (data not shown), and the best resolution was provided by using the Cytofix/Cytoperm reagents from BD PharMingen.

We next examined the expression of perforin in CMV-, EBV-, and flu-specific CD8 T cells. Fig. 6*A* shows the flow cytometric analysis of perforin and Ag specificity in CD8^{high}-gated lymphocytes. Regardless of the type of virus Ag, virtually all the Ag-specific CD8 T cells exhibit significant levels of perforin. The intensity of the staining appears to be more pronounced in CMV-specific cells followed by EBV- and flu-specific cells, respectively. Unlike what is observed in the bulk populations of CD8 T cells, the Ag-specific CD8 T cells exhibit only two subsets of cells with respect to CCR7 and perforin: CCR7^{int}perforin^{low} and CCR7$^-$perforin^{int} (Fig. 6*B*).

The level of perforin detected in CCR7^{int} Ag-specific cells is lower than that found in CCR7$^-$ cells; however, it is significantly higher when compared with the bulk population of naive CD8 T cells of the corresponding donors. It shows from 2- to 5-fold differences in mean fluorescence intensity for perforin between CCR7^{int} Ag-specific cells and naive CD8 T cells (Fig. 6*C*). This result indicates that, although at low level, the central memory CD8 T cells are able to express perforin. Due to limitations in the availability of Ag-specific cells that is a result of their low frequency, we have so far not been able to satisfactorily test the lytic function of sorted CCR7^{int} and CCR7$^-$ populations in chromium-release assays.

Discussion

A number of laboratories studying CD8$^+$ T cell responses in humans have observed that populations of specific cells defined by HLA tetramer staining are often functionally heterogeneous and contain cells that do not produce cytokines detectable in intracellular cytokine staining assays (2–6, 8). Many investigators have interpreted this data in terms of the central and effector memory hypothesis recently introduced by Sallusto et al. (9). This hypothesis proposes that CCR7$^+$ cells constitute a central memory population that is incapable of immediate early effector function but exhibits much greater proliferative activities compared with those of CCR7$^-$ cells, which constitute an effector memory population that is responsible for immediate early effector function.

The central and effector memory hypothesis has gained wide acceptance (2, 6, 16–18), although recently studies have begun to appear refuting at least part of the hypothesis (4, 12). One area of

confusion is that some authors have followed the original approach of identifying the subsets based upon cell surface phenotype (2, 4, 12), while others have instead defined the subsets by their anatomical location (16, 17). Using the anatomic definition in mouse models, both Masopust et al. (16) and Reinhardt et al. (17) found that cells possessing immediate effector functions were preferably located in nonlymphoid tissue, while secondary lymphoid tissues contained memory cells that were either less lytic (16) or did not produce cytokines in short-term Ag stimulation (17); neither of these investigators attempted to correlate these disparate functions with cell surface phenotypes. In human subjects, it is much more difficult to assess the functional characteristics of Ag-specific cells in a variety of lymphoid and nonlymphoid tissues, so most investigators have focused their attention upon cells derived from the peripheral blood that have defined cell surface phenotypes. Even here, the data are in conflict. The work of Champagne et al. (4) clearly demonstrated that >50% of the CCR7$^+$CD8$^+$ cells specific for a HLA-B8-restricted epitope from HIV *nef* are capable of producing IFN-γ in a short-term stimulation assay, although this result did not feature prominently in their discussion. In contrast, Rickinson and coworkers (2) observed that among CD8$^+$A2/GLC$^+$ cells, only the CCR7$^-$ cells were capable of producing IFN-γ in short-term assays. Picker and coworkers (18) have attempted to bridge the gap between anatomy and cell surface phenotype through studies in rhesus macaques, but they base their phenotypic definition upon the expression CD28 instead of CCR7. Although T cells found in nonlymphoid sites were enriched in the CD28$^-$ population, both the CD28$^+$ and CD28$^-$ subsets in peripheral blood were able to produce cytokines in response to staphylococcal enterotoxin B stimulation, a result that is consistent with the observations of Hislop et al. (2) of EBV-specific cells in PBMC in humans.

We set out to determine whether the CCR7 phenotype of Ag-specific CD8$^+$ T cells accounts for the observed functional heterogeneity, thereby also providing a stringent test of one of the important predictions of the central and effector memory hypothesis. We identified Ag-specific cells by HLA tetramer staining, and we subdivided the Ag-specific population into CCR7$^+$ and CCR7$^-$ subsets using a newly developed fluorescent ligand for CCR7, the CCL19 chemotetramer. This approach has turned out to be advantageous over using a conventional mAb for CCR7, as it reveals different levels of CCR7 on memory compared with naive CD8 T cells. The functional studies have revealed that CCR7^{int} Ag-specific memory CD8 T cells produce IFN-γ and TNF-α in a short-term peptide stimulation assay as effectively as their CCR7$^-$ counterparts. Furthermore, the intracellular staining of Ag-specific CD8 T cells before peptide stimulation has revealed that CCR7^{int} memory cells express significant levels of perforin, although it is noticeably lower compared
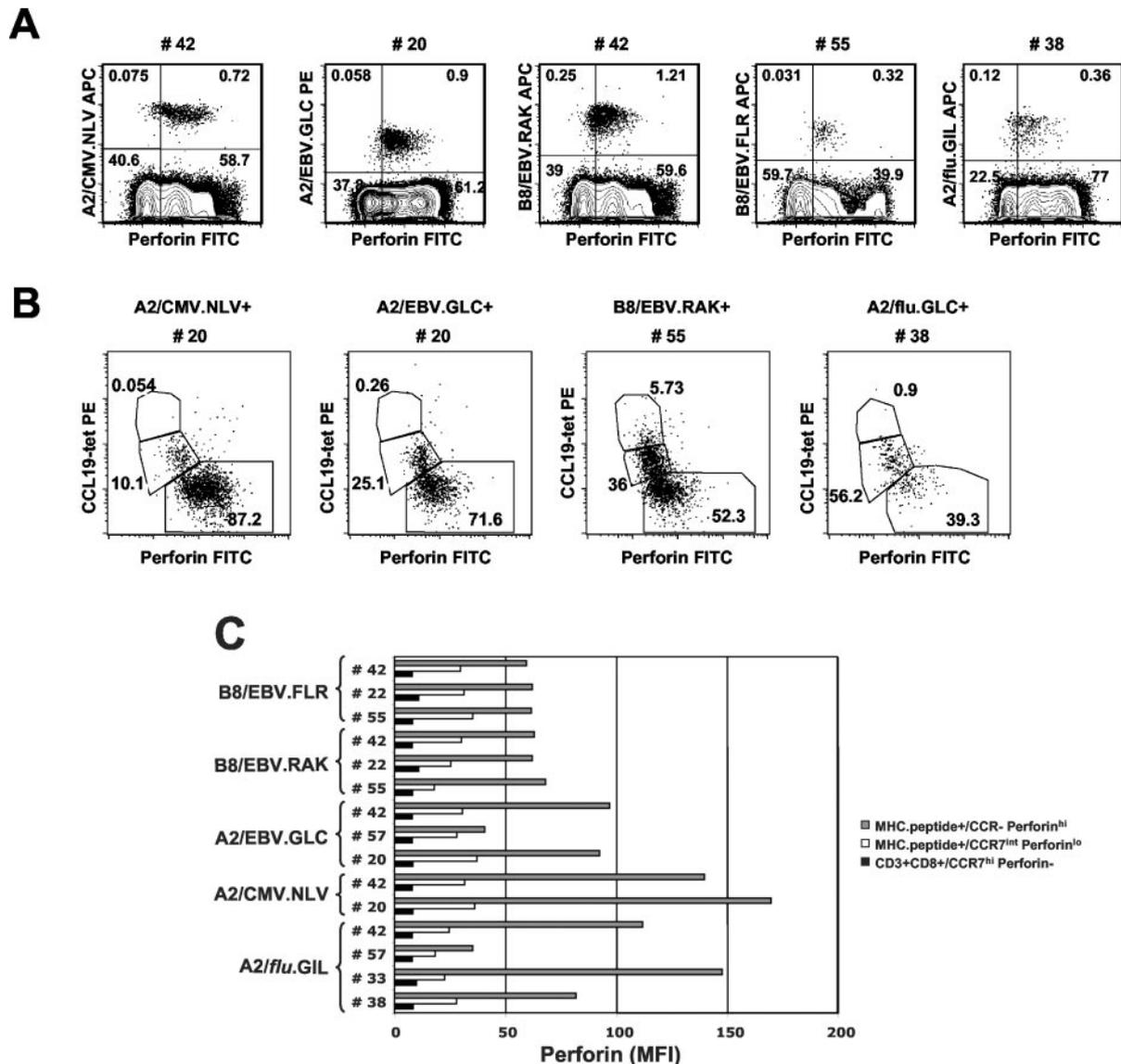
FIGURE 6. Expression of perforin and CCR7 in Ag-specific CD8 T cells. *A*, Shown is the expression of perforin in A2/CMV.NLV-, A2/EBV.GLC-, B8/EBV.RAK-, B8/EBV.FLR-, and A2/flu-specific CD8 T cells (*upper quadrants*) relatively to the level of perforin in the bulk population of CD8 T cells from different donors. *B*, Shown is the relationship between CCR7 and perforin in Ag-specific CD8 T cells. Two subsets of cells can be identified: CCR7^{int}perforin^{low} and CCR7$^-$perforin^{int}. *C*, Shown is a comparison of mean fluorescence intensity for perforin between naive CD8 T cells and the two subsets of Ag-specific CD8 T cells of the corresponding donors.

with that of CCR7$^-$ memory CD8 T cells. The chemotetramer approach that we have taken to identify cells expressing CCR7 should be applicable to other chemokine receptors—and to cell surface receptors in general—and will be particularly attractive when the relevant Abs are not available, as is the case for many chemokine receptors in the mouse. Other laboratories (19, 20) have also recently identified cells expressing chemokine receptors by labeled ligand binding, using fusions of the chemokine to Ig domains.

Explanation for remaining functional heterogeneity

Although our data clearly demonstrate that the heterogeneous capacity of Ag-specific CD8$^+$ T cell populations in humans to rapidly produce IFN-γ is not correlated with the CCR7 phenotype (Figs. 4 and 5), our data do not provide an alternate account for the heterogeneity, when and whether it is observed. The possibilities are 1) the assay methods that we and others (4–6, 8) routinely use may be suboptimal, 2) the population of interest contains cells that respond over a broader dose range than was used in the experiment

(21), and/or 3) the functional heterogeneity may reflect important biological phenomena that has yet to be associated with a defined, purifiable cell subset.

There are a number of genuine biological phenomena that might account for observed functional heterogeneity. It is possible that intermittent exposure to persisting (e.g., herpesviruses such as EBV and CMV) Ag might induce some form of tolerance or impotence. These phenomena have been convincingly observed when the Ag is present continuously and at a high level, such as is observed following infection of CD4-deficient mice with pathogenic strains of lymphocytic choriomeningitis virus (22), in HIV$^+$ patients with high viral loads (23), or during the acute phase of infection with hepatitis C virus (24). However, the Ag burden in each of these cases is probably many orders of magnitude greater than is encountered during intermittent reactivation of a latent herpesvirus.

It is also possible that heterogeneity in the cytokine-producing capacity of Ag-specific CD8$^+$ T cells is due to the existence of subpopulations that are differentially susceptible to apoptosis (25).

In principle, it ought to be possible to work this out by combining techniques for measuring apoptosis with methods developed for costaining with MHC tetramers and Abs against intracellular cytokines (3). In addition, this combination of experiments might require the use of more than the four fluorescence parameters that are available on most analytical flow cytometers. Finally, it is possible that some populations of Ag-specific CD8$^+$ T cells are heterogeneous not in their ability to produce cytokines, but in the pattern of cytokines that they produce (although we and most investigators habitually test for the production of multiple type-I and type-II cytokines). Of course, none of these possibilities are mutually exclusive.

Comparison to other models connecting phenotype/function

The primary significance of the central and effector memory model, or other models that attempt to correlate physical phenotype with function such as the T cell maturation model of Pantaleo and colleagues (4), lies in whether it explains significant in vivo phenomena such as the ability to keep chronic or latent infections in check or to provide protection against reinfection with a pathogen. These questions obviously become exceedingly important for rational vaccine development, where it becomes necessary not only to study the frequency of a T cell population induced by a vaccine, but also to follow the phenotypic distribution of the vaccine-induced T cell subsets over time. This is the easy part. The hard part comes in sorting out the relative contributions during a secondary immune response of distinct phenotypic subsets that have the same Ag specificity. Working this out in humans will be a daunting task because we lack the ability to transfer purified T cell subpopulations into syngeneic hosts, and even if we could, we would not be able to challenge the T cell recipients with relevant pathogens.

Many of these issues should be explored in mouse models, but we must also be cautious about extending the conclusions from these investigations to the human immune system. For example, it is well known that, in the mouse, there are clear and distinct CD62L$^+$ and CD62L$^-$ CD8$^+$ T cell memory populations, and that the relative frequency of the CD62L$^+$ subset among total Ag-specific cells increases over time (26–28). It is also clear that this marker is not associated with heterogeneity in immediate antiviral cytokine responses—this sort of functional heterogeneity generally has not been observed in mouse models (29)—although some investigators believe that the phenotype may be correlated with immediate lytic function (30). Nevertheless, the CD62L$^+$ and CD62L$^-$ memory populations might still play distinct roles in providing protection that are based upon other phenotypic properties of a memory T cell, such as its propensity to traffic to distinct anatomical sites, or its proliferative potential (16). It is certainly possible that some of these properties might be consistent with the teleology suggested by the central and effector memory paradigm.

Acknowledgments

References

1. Altman, J. D., P. A. H. Moss, P. J. R. Goulder, D. H. Barouch, M. G. McHeyzer-Williams, J. I. Bell, A. J. McMichael, and M. M. Davis. 1996. Phenotypic analysis of antigen-specific T lymphocytes. *Science 274:94.*
2. Hislop, A. D., N. H. Gudgeon, M. F. C. Callan, C. Fazou, H. Hasegawa, M. Salmon, and A. B. Rickinson. 2001. EBV-specific CD8$^+$ T cell memory: relationships between epitope specificity, cell phenotype, and immediate effector function. *J. Immunol. 167:2019.*
3. Appay, V., D. F. Nixon, S. M. Donahoe, G. M. Gillespie, T. Dong, A. King, G. S. Ogg, H. M. Spiegel, C. Conlon, C. A. Spina, et al. 2000. HIV-specific

4. Champagne, P., G. S. Ogg, A. S. King, C. Knabenhans, K. Ellefsen, M. Nobile, V. Appay, G. P. Rizzardi, S. Fleury, M. Lipp, et al. 2001. Skewed maturation of memory HIV-specific CD8 T lymphocytes. *Nature 410:106.*
5. Gillespie, G. M., M. R. Wills, V. Appay, C. O'Callaghan, M. Murphy, N. Smith, P. Sissons, S. Rowland-Jones, J. I. Bell, and P. A. Moss. 2000. Functional heterogeneity and high frequencies of cytomegalovirus-specific CD8$^+$ T lymphocytes in healthy seropositive donors. *J. Virol. 74:8140.*
6. Tussey, L., S. Speller, A. Gallimore, and R. Vessey. 2000. Functionally distinct CD8$^+$ memory T cell subsets in persistent EBV infection are differentiated by migratory receptor expression. *Eur. J. Immunol. 30:1823.*
7. Ogg, G. S., X. Jin, S. Bonhoeffer, P. R. Dunbar, M. A. Nowak, S. Monard, J. P. Segal, Y. Cao, S. L. Rowland-Jones, V. Cerundolo, et al. 1998. Quantitation of HIV-1-specific cytotoxic T lymphocytes and plasma load of viral RNA. *Science 279:2103.*
8. Sandberg, J. K., N. M. Fast, and D. F. Nixon. 2001. Functional heterogeneity of cytokines and cytolytic effector molecules in human CD8$^+$ T lymphocytes. *J. Immunol. 167:181.*
9. Sallusto, F., D. Lenig, R. Forster, M. Lipp, and A. Lanzavecchia. 1999. Two subsets of memory T lymphocytes with distinct homing potentials and effector functions. *Nature 401:708.*
10. Murphy, P. M., M. Baggiolini, I. F. Charo, C. A. Hebert, R. Horuk, K. Matsushima, L. H. Miller, J. J. Oppenheim, and C. A. Power. 2000. International union of pharmacology. XXII. Nomenclature for chemokine receptors. *Pharmacol. Rev. 52:145.*
11. Zlotnik, A., and O. Yoshie. 2000. Chemokines: a new classification system and their role in immunity. *Immunity 12:121.*
12. Unsoeld, H., S. Krautwald, D. Voehringer, U. Kunzendorf, and H. Pircher. 2002. Cutting edge: CCR7$^+$ and CCR7$^-$ memory T cells do not differ in immediate effector cell function. *J. Immunol. 169:638.*
13. Yoshida, R., M. Nagira, M. Kitaura, N. Imagawa, T. Imai, and O. Yoshie. 1998. Secondary lymphoid-tissue chemokine is a functional ligand for the CC chemokine receptor CCR7. *J. Biol. Chem. 273:7118.*
14. Callan, M. F., L. Tan, N. Annels, G. S. Ogg, J. D. Wilson, C. A. O'Callaghan, N. Steven, A. J. McMichael, and A. B. Rickinson. 1998. Direct visualization of antigen-specific CD8$^+$ T cells during the primary immune response to Epstein-Barr virus in vivo. *J. Exp. Med. 187:1395.*
15. Barry, M., and R. C. Bleackley. 2002. Cytotoxic T lymphocytes: all roads lead to death. *Nat. Rev. Immunol. 2:401.*
16. Masopust, D., V. Vezys, A. L. Marzo, and L. Lefrancois. 2001. Preferential localization of effector memory cells in nonlymphoid tissue. *Science 291:2413.*
17. Reinhardt, R. L., A. Khoruts, R. Merica, T. Zell, and M. K. Jenkins. 2001. Visualizing the generation of memory CD4 T cells in the whole body. *Nature 410:101.*
18. Pitcher, C. J., S. I. Hagen, J. M. Walker, R. Lum, B. L. Mitchell, V. C. Maino, M. K. Axthelm, and L. J. Picker. 2002. Development and homeostasis of T cell memory in rhesus macaque. *J. Immunol. 168:29.*
19. Manjunath, N., P. Shankar, J. Wan, W. Weninger, M. A. Crowley, K. Hieshima, T. A. Springer, X. Fan, H. Shen, J. Lieberman, and U. H. von Andrian. 2001. Effector differentiation is not prerequisite for generation of memory cytotoxic T lymphocytes. *J. Clin. Invest. 108:871.*
20. Hargreaves, D. C., P. L. Hyman, T. T. Lu, V. N. Ngo, A. Bidgol, G. Suzuki, Y.-R. Zou, D. R. Littman, and J. G. Cyster. 2001. A coordinated change in chemokine responsiveness guides plasma cell movements. *J. Exp. Med. 194:45.*
21. Bitmansour, A. D., D. C. Douek, V. C. Maino, and L. J. Picker. 2002. Direct ex vivo analysis of human CD4$^+$ memory T cell activation requirements at the single clonotype level. *J. Immunol. 169:1207.*
22. Zajac, A. J., J. N. Blattman, K. Murali-Krishna, D. J. Sourdive, M. Suresh, J. D. Altman, and R. Ahmed. 1998. Viral immune evasion due to persistence of activated T-cells without effector function. *J. Exp. Med. 188:2205.*
23. Kostense, S., G. S. Ogg, E. H. Manting, G. Gillespie, J. Joling, K. Vandenberghe, E. Z. Veenhof, D. van Baarle, S. Jurriaans, M. R. Klein, and F. Miedema. 2001. High viral burden in the presence of major HIV-specific CD8$^+$ T cell expansions: evidence for impaired CTL effector function. *Eur. J. Immunol. 31:677.*
24. Lechner, F., D. K. Wong, P. R. Dunbar, R. Chapman, R. T. Chung, P. Dohrenwend, G. Robbins, R. Phillips, P. Klenerman, and B. D. Walker. 2000. Analysis of successful immune responses in persons infected with hepatitis C virus. *J. Exp. Med. 191:1499.*
25. Mueller, Y. M., S. C. De Rosa, J. A. Hutton, J. Witek, M. Roederer, J. D. Altman, and P. D. Katsikis. 2001. Increased CD95/Fas-induced apoptosis of HIV-specific CD8$^+$ T cells. *Immunity 15:871.*
26. Tripp, R. A., S. Hou, and P. C. Doherty. 1995. Temporal loss of the activated L-selectin-low phenotype for virus-specific CD8$^+$ memory T cells. *J. Immunol. 154:5870.*
27. Zimmerman, C., K. Brduscha-Riem, C. Blaser, R. M. Zinkernagel, and H. Pircher. 1996. Visualization, characterization, and turnover of CD8$^+$ memory T cells in virus-infected hosts. *J. Exp. Med. 183:1367.*
28. Busch, D. H., I. M. Pilip, S. Vijh, and E. G. Pamer. 1998. Coordinate regulation of complex T cell populations responding to bacterial infection. *Immunity 8:353.*
29. Murali-Krishna, K., J. D. Altman, M. Suresh, D. J. Sourdive, A. J. Zajac, J. D. Miller, J. Slansky, and R. Ahmed. 1998. Counting antigen-specific CD8 T cells: a reevaluation of bystander activation during viral infection. *Immunity 8:177.*
30. Oehen, S., and K. Brduscha-Riem. 1998. Differentiation of naive CTL to effector and memory CTL: correlation of effector function with phenotype and cell division. *J. Immunol. 161:5338.*

CD8$^+$ T cells produce antiviral cytokines but are impaired in cytolytic function. *J. Exp. Med. 192:63.*